Cor et Vasa

Available online at www.sciencedirect.com

ScienceDirect

journal homepage: www.elsevier.com/locate/crvasa

Přehledový článek | Review article

Intravascular ultrasound, optical coherence tomography and near infrared spectroscopy

Tomasz Roleder, Wojciech Wojakowski

3rd Department of Cardiology, Medical University of Silesia in Katowice, Katowice, Poland

ARTICLE INFO

Article history:
Received: 14. 8. 2015
Received in revised form: 5. 10. 2015
Accepted: 6. 10. 2015
Available online: 6. 11. 2015

Klíčová slova:
Blízká infračervená spektroskopie
Intravaskulární ultrazvuk
Optická koherenční tomografie

Keywords:
Intravascular ultrasound
Near infrared spectroscopy
Optical coherence tomography

SOUHRN

Intravaskulární ultrazvuk (IVUS), optická koherenční tomografie (OCT) a blízká infračervená spektroskopie (near infrared spectroscopy, NIRS) umožňují detailní *in vivo* analýzu morfologie ateromu. Navíc pomáhají vést intervenci v koronárních tepnách a zhodnotit výsledek implantace stentu. Metody IVUS, OCT a NIRS poskytují jedinečné údaje o analyzované tkáni, a tak se navzájem doplňují. Jejich použití v každodenní klinické praxi pomáhá rozpoznat příčinu onemocnění a mohou přispět ke zlepšení výsledku intervencí v koronárních tepnách.

ABSTRACT

Intravascular ultrasound (IVUS), optical coherence tomography (OCT) and near infrared spectroscopy (NIRS) allow for a thorough analysis of the atheroma's morphology *in vivo*. Moreover, it helps to guide coronary intervention and assess the results of stenting. IVUS, OCT and NIRS provide unique data about the analyzed tissue and thus all of them complement each other. Their application in daily clinical practice helps to understand the underlying pathology of disease and may contribute to the improvement of outcomes in coronary interventions.

Introduction

The introduction of intravascular imaging opened new horizons for the presentation of coronary atherosclerosis *in vivo*. It became possible to follow the development of atherosclerosis and to detect atheromas that are prone to rupture (vulnerable plaques) known as thin fibrous cap atheromas (TCFA). Moreover, intravascular imaging helps to guide coronary interventions and to assess their results. Nowadays, available intravascular imaging modalities utilize ultrasound and near infrared light (niR). Due to their intrinsic properties, both ultrasound and niR deliver unique information about the analyzed tissue and thus complement each other. The following review presents the basics of intravascular ultrasound (IVUS), optical coherence tomography (OCT) and niR spectroscopy (NIRS) in terms of plaque description, percutaneous coronary intervention (PCI) guidance and clinical application.

Intravascular ultrasound

The intravascular ultrasound (IVUS) is an invasive imaging modality that utilizes ultrasound (20–40 MHz) to present the vessel wall [1]. The dedicated IVUS catheter is advanced into the coronary vessel over a guidewire. The procedure is

Address: Tomasz Roleder MD, PhD, 3rd Department of Cardiology, Medical University of Silesia in Katowice, 45/47 Ziolowa street, 40-635 Katowice, Poland, e-mail: tomaszroleder@gmail.com
DOI: 10.1016/j.crvasa.2015.10.004

Please cite this article as: T. Roleder, W. Wojakowski, Intravascular ultrasound, optical coherence tomography and near infrared spectroscopy, Cor et Vasa 57 (2015) e439–e445 as published in the online version of *Cor et Vasa* available at http://www.sciencedirect.com/science/article/pii/S0010865015001083

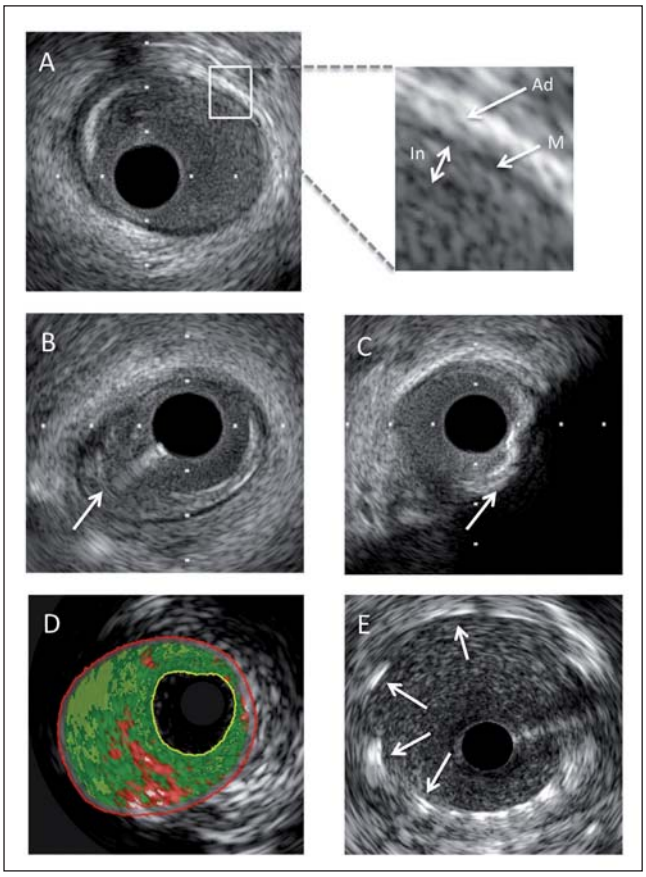

Fig. 1 – Representative images of intravascular ultrasound (IVUS). (A) Cross-sectional gray-scale IVUS (40 MHz probe) image of the healthy segment of coronary artery presenting the intima (In), the media (M) and the adventitia (Ad). (B) Cross-sectional gray-scale IVUS (40 MHz probe) image of the soft plaque (white arrow). (C) Cross-sectional gray-scale IVUS (40 MHz probe) image of calcification (white arrow). (D) Cross-sectional virtual histology IVUS image (20 MHz probe) of thick fibroatheroma. Plaque burden is a space between the yellow line and red line expressed as percentage of area bordered by red line. (E) Cross-sectional gray-scale IVUS (20 MHz probe) image after stent implantation presenting appropriate stent struts apposition (white arrows).

usually performed as part of standard invasive diagnostic coronary angiography. The IVUS probe is pulled back in the coronary vessel with a constant speed (1 or 0.5 mm/s) and simultaneously provides gray-scale cross-sectional and longitudinal images of the analyzed vessel. The axial resolution of IVUS ranges from 100 to 200 μm, which allows presenting three layers of the vessel at cross-sectional images: intima, media and adventitia. The lumen area, vessel area, plaque burden (the amount of plaque that occupies vessel area) and plaque volume are estimated by IVUS (Fig. 1). Moreover, the IVUS longitudinal analysis describes vessel remodeling. If the maximal vessel area within the plaque is higher than the vessel reference area, the positive vessel remodeling occurs. If maximal vessel area is lower than the vessel size, the lesion is classified as negatively remodeled [2]. Nevertheless, the plaque composition is roughly estimated by gray-scale IVUS. The echo-lucent plaque with shadowing is described as calcified [3] whereas plaques with low echogenity are described as soft and their composition remains unclear [4] (Fig. 1).

More precise analysis of soft plaque composition by IVUS is derived by spectral analysis of its signal, known as Virtual Histology (VH-IVUS). VH-IVUS identifies 4 different types of plaque components: fibrous (green), fibro-fatty (yellow), dense calcium (white) and necrotic core (red) [5] (Fig. 1). Its accuracy has been documented by *in vivo* and *in vitro* studies. Moreover, VH-IVUS is able to detect thin fibrous cap atheroma (TCFA). TCFA is covered with fibrous cap less then 65 μm thick and IVUS resolution does not allow for direct measurement of cap thickness. Hence, the plaque is recognized as TCFA by VH-IVUS if the necrotic core (red color) has a direct contact with the lumen and occupies more then 40% of the plaque in 3 consecutive cross-sectional images. The PROSPECT study showed that the presence of such recognized TCFA increases the risk of future coronary events [6]. However, the results of the PROSPECT study should be discussed in light of controversies around precision of VH-IVUS. The histology data suggested poor accuracy of VH-IVUS in the necrotic core detection [7].

For many years IVUS imaging also served as a tool to estimate the significance of the intermediate coronary artery stenosis. The cut-off value of lumen area for non-left main (LM) stenosis was 4 mm^2 [8]. However, reports comparing the results of FFR and IVUS suggested that such cut-off value should be less then 3.07 mm^2 in non-LM stenosis, and less then 5.5 mm^2 in LM stenosis [9]. Nowadays, it is only appropriate to assess the significance of LM stenosis by IVUS, and despite the results of FFR studies clinical observations suggest that 6 mm^2 lumen area is the most appropriate cut-off value [10].

IVUS also helps to guide coronary interventions. Obtained measurements of the treated plaque facilitate the choice of appropriate stent diameter and length, and to assess the results of stenting (Fig. 1). IVUS easily presents stent under-expansion, stent malappositon and vessel dissection – three main risk factors for the acute stent thrombosis [11]. It is suggested that the optimal minimal DES area should be more then 8 mm^2 in LM, more than 6 mm^2 in proximal segment of LAD, and more then 5 mm^2 in proximal segment of Cx post procedure [12]. IVUS guided PCI significantly decreases all-cause mortality in both left main and non-left main stenting [13–15].

Optical coherence tomography

Similarly to IVUS, OCT provides cross-sectional images of the vessel. Instead of ultrasound OCT utilizes niR to present the morphology of the vessel; niR wavelength ranges between 1250 and 1350 nm. niR is split in two paths and the signal is obtained from the interference of the light backscattered from the analyzed tissue with the light backscattered from the reference mirror [16]. Initially OCT imaging used time-domain (TD) slow analysis of the interference signal. Currently it has been replaced with much faster frequency domain (FD) analysis, which significantly speed up the imaging process [17].

As opposed to the IVUS imaging, the utilization of niR for OCT imaging requires blood removal from the vessel at the time of imaging, as the wavelength of niR does not penetrate through red blood cells. First TD OCT systems

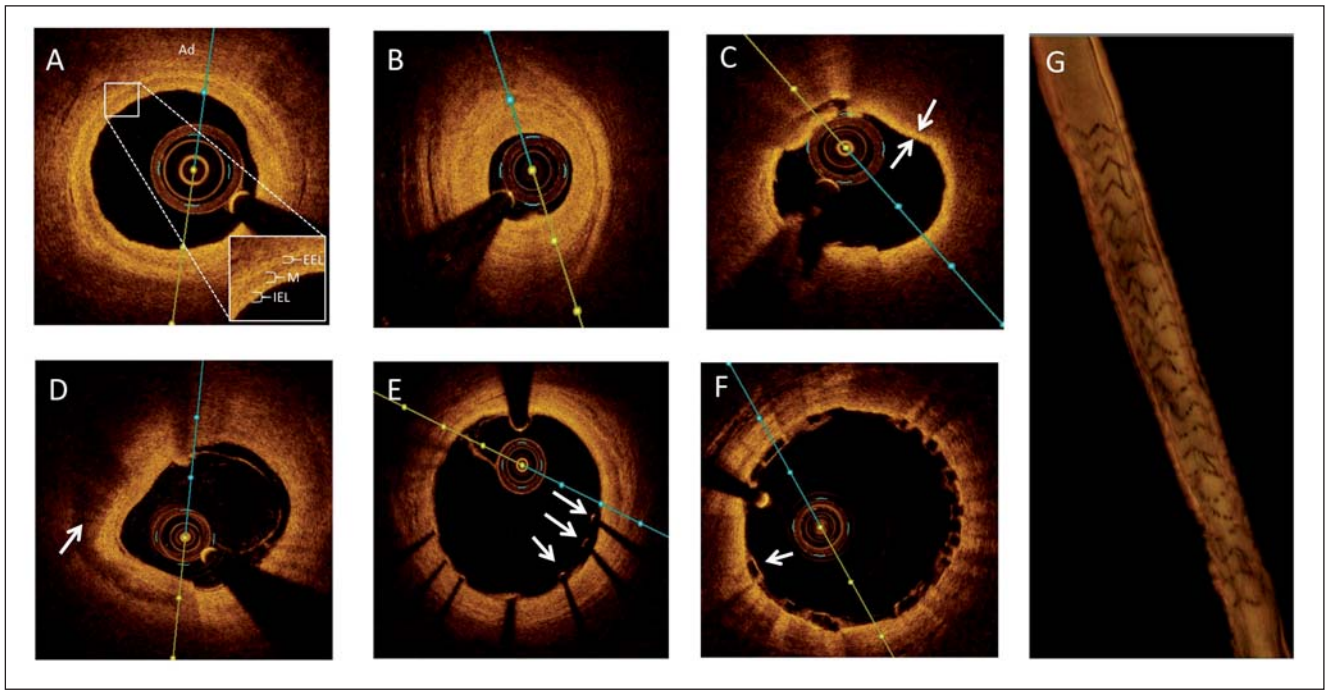

Fig. 2 – Representative images of intravascular optical coherence imaging (OCT). (A) Cross-sectional OCT image of healthy segment of coronary vessel presenting the internal elastic lamina (IEL), the media (M), external elastic lamina (EEL) and adventitia (Ad). (B) Cross-sectional OCT image of fibrotic lesions. (C) Cross-sectional OCT image of lipid-rich lesion covered with thin fibrous cap atheroma (TCFA – white arrows). The image presents also small red thrombi. (D) Cross-sectional OCT image of calcification (white arrow). (E) Cross-sectional OCT image after the implantation of the everolimus eluting stent with visible stent struts in malapposition (white arrows). (F) Cross-sectional OCT image post implantation of bioabsorbable vascular scaffold with visible polymeric struts. (G) Three-dimensional reconstruction of coronary artery at the site of stent implantation.

required coronary artery occlusion at the time of imaging, which increased the risk of life threatening arrhythmias. The now-available FD-OCT imaging systems are so fast that the procedure may be performed at the time of a 3 s long injection of the contrast agent [18], which makes the procedure much safer [19].

OCT system is composed of the workstation and intravascular catheters with the OCT probe. The catheters are monorail systems and are advanced over a guidewire to the coronary artery. At the time of imaging the contrast is injected to flush the blood away and the probe is pulled back from distal segment to proximal segment of the artery. OCT imaging lasts 2.7 s and presents from 54 (10 μm step) to 72 mm (13 μm step) of the vessel length during the single pullback of the probe.

The use of light significantly improved the resolution of intravascular imaging. It ranges between 10 and 20 μm. However, the improved resolution is at the cost of beam penetration into the vessel wall. It obtains a signal only from 1 to 3 mm of the vessel wall, and thus does not allow to present plaque burden, and consequently plaque volume and vessel remodeling [17].

Nevertheless, similarly to IVUS, OCT provides quantitative analysis of the vessel lumen and OCT automated contour detection is very accurate and allows a very precise measurement of lumen area, lumen diameter and length of region of interest. Moreover, a novel OCT system (iLumien Optis, St Jude Medical) provides an automated three-dimensional reconstruction of the analyzed segment (Fig. 2), which is overlaid on the angiography image to precisely guide PCI [20].

In healthy segments of coronary artery OCT presents four layers of the arterial wall: inter-elastic lamina, media, external elastic lamina and adventitia (Fig. 2). At the site of atheroma OCT is able to distinguish lipid, fibrotic and calcified components of the analyzed tissue. The lipid is characterized by high signal attenuation with the diffuse edges, calcium – by signal-poor area with sharp borders, and fibrotic components are presented as homogenous tissue with high reflectivity [21]. The high accuracy of plaque composition delivered by OCT was confirmed by histology [22] (Fig. 2). OCT is also able to present thrombus (and differentiate white thrombus from red one), intimal tear, intramural hematoma, micro vessels, and macrophage [17].

Thanks to high resolution of OCT imaging it became possible to directly measure the thickness of the fibrotic cap covering the lipid core and thus to detect TCFA. It makes OCT the gold standard to detect vulnerable plaques [23] (Fig. 2).

High resolution of OCT imaging enables to present the results of coronary intervention with the unprecedented precision. The stent strut malapposition, stent under-expansion and vessel dissection are very clearly presented by OCT. Due to light properties, metallic struts are only visible at their adluminal edge, and the knowledge about the strut thickness is necessary for stent apposition assessment. If the distance between the middle of the blooming struts and the vessel contour is more than the strut thickness, the malapposition is detected [24] (Fig. 2). Contrary to metallic stents, the whole polymeric struts of bioresorbable vascular scaffolds (BVS) are presented by OCT and malappositon

is easily detected as a gap between the scaffold and the vessel contour. BVS imaging by OCT is also able to present a scaffold disruption, which is not possible to detect by fluoroscopy [25]. Notably, OCT is the only method that can appropriately assess the expansion of BVS.

In addition to the stent apposition, OCT presents plaque protrusion through stent struts and thrombus formation.

OCT has been broadly applied in the assessment of vessel healing after stent implantation. It perfectly presents stent struts coverage by neointima and provides neointima characteristic [26]. The heterogenous, layered, homogenous and lipid rich neointima may be described by OCT within implanted stent and at follow-up. The lack of homogenous neointima is associated with poorer clinical outcome [27]. Lipid-rich neointima indicates the presence of neoatherosclerosis within the stent, the heterogenous neointima is associated with high amount of fibrin, and layered neointima with persistent peri-struts inflammation [28].

OCT imaging also provides new approach in the treatment of myocardial infraction. It distinguishes between plaque rupture and plaque erosion as a cause of vascular thrombosis. Initial clinical observations suggest that eroded plaque may be subjected only to thrombectomy and left unstented without any major adverse cardiac events observed during the long-term follow-up [29].

Near infrared spectroscopy

NIRS utilizes niR in a range between 780 and 2500 μm to analyze the molar absorptivity of the tissue. Since light is absorbed with a different degree for every single particle, NIRS is able to present the chemical composition of the analyzed object. NIRS has been introduced into coronary imaging as modality focused on the detection of lipid deposition within the vessel [30]. As opposed to OCT, the applied wavelength of niR does not require blood removal from the vessel lumen to perform the analysis. Moreover, the intravascular NIRS is the only tool to assess tissue composition through the eyes of the implanted stent struts [31].

Similar to OCT and IVUS, the NIRS system is composed of an off-line station and intravascular catheters, which contain NIRS probe. NIRS probe is advanced into region of interest and pulled back with a speed 0.5 mm/s. NIRS penetration into the vessel wall is about 1 mm. Raw spectra of NIRS are decoded into a 7-digit color map and a 7-digit color block chemogram. A lipid distribution over the vessel is presented as yellow, tan and orange pixels whereas red pixels indicate its absence. If a pixel does not contain enough data (e.g. as caused by a guidewire), it appears black. The X-axis on the NIRS map presents the length of the pullback and the Y-axis on the map presents vessel circumference in degrees (0–360°) (Fig. 3).

NIRS mapping allows calculation of lipid core burden index (LCBI). It is a rate of all yellow pixels within the analysed segment and is expressed per mille. LCBI is calculated for the total length of the region of interest, and the 4 mm segment with the highest LCBI ($LCBI_{4mm}$) is emphasized. The NIRS block chemogram presents the probability of lipid deposition within 2 mm segments. For both NIRS map and NIRS chemogram the yellow indicates >0.97, tan indicates 0.84–0.97, orange indicates 0.57–0.83 and red indicates < 0.57 probability of lipid deposition. In summary, NIRS map is a very simple picture with lipids presented as yellow pixels on the red background. The presentation of lipid deposition by NIRS map and block chemogram has been validated by the histology [32] (Fig. 3).

In current practice NIRS has been only applied for research purposes and does not have any clinical applica-

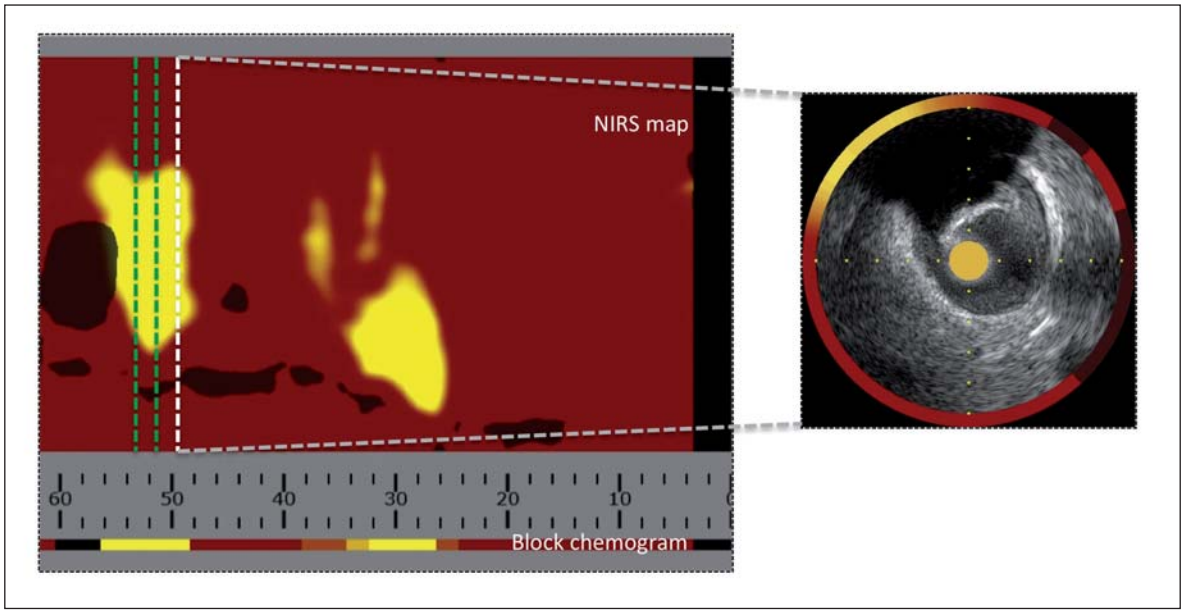

Fig. 3 – Representative image of intravascular near infrared spectroscopy (NIRS) combined with IVUS image. The figure presents NIRS map with detected lipids (yellow color) and the NIRS block chemogram. Black pixels present the region with not enough data to analysis. Green dashed arrows present the segment of the vessel with the highest lipid-core burden index = 283. The white dashed line corresponds to the cross-sectional image of IVUS with overlayed NIRS map as a colourful ring.

tion. YELLOW study found that with the use of NIRS one may observe chemical reconstruction of the plaque subjected to aggressive lipid-lowering therapy [33]. COLOR registry suggested that stenting of lesions with $LCBI_{4mm}$ > 500 constitutes a risk of peri-procedural myocardial infarction [34], but CANARY did not find any benefits to patients from the use of distal protection devices during PCI of lesion with $LCBI_{4mm}$ > 600 [35,36]. The on-going LRP study is aimed to estimate whether NIRS coronary imaging may help to predict the future coronary events.

Finally, NIRS probe has been combined with the gray-scale IVUS to present the morphology of the lesion more precisely (Fig. 3). It is now the only hybrid intravascular imaging catheter available on the market. The results of IVUS and NIRS imaging are overlaid against each other and the combined IVUS and NIRS cross-sectional image is displayed. The NIRS ring at the cross-sectional NIRS-IVUS image corresponds to the location at the NIRS map (Fig. 3). The combination of both modalities enriched the gray-scale IVUS analysis with NIRS. Results from the histology showed that combined IVUS-NIRS analysis poses a high accuracy in detection of fibroatheromas [4]. On the other hand clinical observation suggested that NIRS-IVUS made possible detection of OCT defined TCFA as positively remodelled vessel with $LCBI_{2mm}$ > 315 [37].

IVUS vs. OCT vs. NIRS

As opposed to IVUS, OCT requires blood removal from the vessel at the time of imaging. It does not allow for ostial lesion assessment. Moreover, OCT requires additional contrast injection and should be used with caution in patients with renal insufficiency. Smaller diameters and lumen areas are also provided by OCT as compared to IVUS measurements. The difference falls between 10% and 20%; thus IVUS cut-off values of lumen area cannot be used in OCT imaging to assess significance of coronary stenosis [38].

In terms of lipid detection, NIRS and OCT correlate moderately [39] and NIRS and VH-IVUS correlate poorly [40]. The correlation between NIRS and VH-IVUS is also poor in calcified lesions [36]. On the other hand, the comparison of TCFA detection by VH-IVUS with OCT defined TCFA show that VH-IVUS overestimate the number of vulnerable plaques [41].

Finally, the analysis from multimodality imaging (OCT, IVUS, NIRS) suggests that OCT derived TCFA is the strongest predictor of distal embolization as compared do LCBI values and plaque burden [42].

Conclusion

Every intravascular imaging modality offers quantitative analysis of the lesion and implanted stent, and provides unique information about the plaque composition and vessel healing. The use of IVUS, OCT and NIRS helps to clarify clinical problems and to guide coronary intervention. It seems that modern invasive cardiology should exploit more intravascular imaging techniques on a daily clinical basis to improve patients' outcomes.

Conflict of interest
No conflict of interest.

Funding body
None.

Ethical statement
Authors state that the research was conducted according to ethical standards.

Acknowledgements
We thank Professor Michal Tendera for provided help during the research (e.g., providing language help, writing assistance or proof reading the article, etc.).

References

[1] P.G. Yock, D.T. Linker, Intravascular ultrasound. Looking below the surface of vascular disease, Circulation 81 (1990) 1715–1718.
[2] A. Shiran, G.S. Mintz, B. Leiboff, et al., Serial volumetric intravascular ultrasound assessment of arterial remodeling in left main coronary artery disease, American Journal of Cardiology 83 (1999) 1427–1432.
[3] M. Meine, A. Machraoui, G. Dasbach, et al., Intravascular ultrasound findings in calcifying arteriosclerosis: in vitro validation using "soft" roentgen images, Zeitschrift für Kardiologie 86 (1997) 818–826.
[4] S.J. Kang, G.S. Mintz, J. Pu, et al., Combined IVUS and NIRS detection of fibroatheromas: histopathological validation in human coronary arteries, Journal of the American College of Cardiology: Cardiovascular Imaging 8 (2015) 184–194.
[5] A. Nair, B.D. Kuban, E.M. Tuzcu, et al., Coronary plaque classification with intravascular ultrasound radiofrequency data analysis, Circulation 106 (2002) 2200–2206.
[6] G.W. Stone, A. Maehara, A.J. Lansky, et al., A prospective natural-history study of coronary atherosclerosis, New England Journal of Medicine 364 (2011) 226–235.
[7] J.F. Granada, D. Wallace-Bradley, H.K. Win, et al., In vivo plaque characterization using intravascular ultrasound-virtual histology in a porcine model of complex coronary lesions, Arteriosclerosis, Thrombosis, and Vascular Biology 27 (2007) 387–393.
[8] C. Briguori, A. Anzuini, F. Airoldi, et al., Intravascular ultrasound criteria for the assessment of the functional significance of intermediate coronary artery stenoses and comparison with fractional flow reserve, American Journal of Cardiology 87 (2001) 136–141.
[9] R. Waksman, J. Legutko, J. Singh, et al., First: fractional flow reserve and intravascular ultrasound relationship study, Journal of the American College of Cardiology 61 (2013) 917–923.
[10] P. Kolh, S. Windecker, F. Alfonso, et al., 2014 ESC/EACTS guidelines on myocardial revascularization: the Task Force on Myocardial Revascularization of the European Society of Cardiology (ESC) and the European Association for Cardio-Thoracic Surgery (EACTS) developed with the special contribution of the European Association of Percutaneous Cardiovascular Interventions (EAPCI), European Heart Journal 35 (2014) 2541–2619.
[11] F. Prati, T. Kodama, E. Romagnoli, et al., Suboptimal stent deployment is associated with subacute stent thrombosis: optical coherence tomography insights from a multicenter matched study. From the CLI Foundation investigators: The CLI-THRO study, American Heart Journal 169 (2015) 249–256.
[12] S.J. Kang, J.M. Ahn, H. Song, et al., Comprehensive intravascular ultrasound assessment of stent area and its impact on restenosis and adverse cardiac events in 403 patients with unprotected left main disease, Circulation: Cardiovascular Interventions 4 (2011) 562–569.

[13] S.J. Park, Y.H. Kim, D.W. Park, et al., Impact of intravascular ultrasound guidance on long-term mortality in stenting for unprotected left main coronary artery stenosis, Circulation: Cardiovascular Interventions 2 (2009) 167–177.
[14] H. Parise, A. Maehara, G.W. Stone, et al., Meta-analysis of randomized studies comparing intravascular ultrasound versus angiographic guidance of percutaneous coronary intervention in pre-drug-eluting stent era, American Journal of Cardiology 107 (2011) 374–382.
[15] B. Witzenbichler, A. Maehara, G. Weisz, et al., Relationship between intravascular ultrasound guidance and clinical outcomes after drug-eluting stents: the assessment of dual antiplatelet therapy with drug-eluting stents (ADAPT-DES) study, Circulation 129 (2014) 463–470.
[16] D. Huang, E.A. Swanson, C.P. Lin, et al., Optical coherence tomography, Science 254 (1991) 1178–1181.
[17] F. Prati, M.W. Jenkins, A. Di Giorgio, A.M. Rollins, Intracoronary optical coherence tomography, basic theory and image acquisition techniques, International Journal of Cardiovascular Imaging 27 (2011) 251–258.
[18] M. Choma, M. Sarunic, C. Yang, J. Izatt, Sensitivity advantage of swept source and Fourier domain optical coherence tomography, Optics Express 11 (2003) 2183–2189.
[19] T. Yamaguchi, M. Terashima, T. Akasaka, et al., Safety and feasibility of an intravascular optical coherence tomography image wire system in the clinical setting, American Journal of Cardiology 101 (2008) 562–567.
[20] L.S. Athanasiou, C.V. Bourantas, P.K. Siogkas, et al., 3D reconstruction of coronary arteries using frequency domain optical coherence tomography images and biplane angiography. Conference proceedings: ... Annual International Conference of the IEEE Engineering in Medicine and Biology Society 2012 (2012) 2647–2650.
[21] H. Yabushita, B.E. Bouma, S.L. Houser, et al., Characterization of human atherosclerosis by optical coherence tomography, Circulation 106 (2002) 1640–1645.
[22] J. Rieber, O. Meissner, G. Babaryka, et al., Diagnostic accuracy of optical coherence tomography and intravascular ultrasound for the detection and characterization of atherosclerotic plaque composition in ex-vivo coronary specimens: a comparison with histology, Coronary Artery Disease 17 (2006) 425–430.
[23] J. Narula, M. Nakano, R. Virmani, et al., Histopathologic characteristics of atherosclerotic coronary disease and implications of the findings for the invasive and noninvasive detection of vulnerable plaques, Journal of the American College of Cardiology 61 (2013) 1041–1051.
[24] H.G. Bezerra, M.A. Costa, G. Guagliumi, et al., Intracoronary optical coherence tomography: a comprehensive review clinical and research applications, Journal of the American College of Cardiology: Cardiovascular Interventions 2 (2009) 1035–1046.
[25] J. Gomez-Lara, M. Radu, S. Brugaletta, et al., Serial analysis of the malapposed and uncovered struts of the new generation of everolimus-eluting bioresorbable scaffold with optical coherence tomography, Journal of the American College of Cardiology: Cardiovascular Interventions 4 (2011) 992–1001.
[26] A. Murata, D. Wallace-Bradley, A. Tellez, et al., Accuracy of optical coherence tomography in the evaluation of neointimal coverage after stent implantation, Journal of the American College of Cardiology: Cardiovascular Imaging 3 (2010) 76–84.
[27] T. Kubo, T. Imanishi, H. Kitabata, et al., Comparison of vascular response after sirolimus-eluting stent implantation between patients with unstable and stable angina pectoris: a serial optical coherence tomography study, Journal of the American College of Cardiology: Cardiovascular Imaging 1 (2008) 475–484.
[28] J.S. Kim, M.E. Afari, J. Ha, et al., Neointimal patterns obtained by optical coherence tomography correlate with specific histological components and neointimal proliferation in a swine model of restenosis, European Heart Journal: Cardiovascular Imaging 15 (2014) 292–298.
[29] F. Prati, S. Uemura, G. Souteyrand, et al., Oct-based diagnosis and management of STEMI associated with intact fibrous cap, Journal of the American College of Cardiology: Cardiovascular Imaging 6 (2013) 283–287.
[30] P.R. Moreno, R.A. Lodder, K.R. Purushothaman, et al., Detection of lipid pool, thin fibrous cap, and inflammatory cells in human aortic atherosclerotic plaques by near-infrared spectroscopy, Circulation 105 (2002) 923–927.
[31] Z.A. Ali, T. Roleder, J. Narula, et al., Increased thin-cap neoatheroma and periprocedural myocardial infarction in drug-eluting stent restenosis: multimodality intravascular imaging of drug-eluting and bare-metal stents, Circulation: Cardiovascular Interventions 6 (2013) 507–517.
[32] S. Waxman, S.R. Dixon, P. L'Allier, et al., In vivo validation of a catheter-based near-infrared spectroscopy system for detection of lipid core coronary plaques: initial results of the spectacle study, Journal of the American College of Cardiology: Cardiovascular Imaging 2 (2009) 858–868.
[33] A.S. Kini, U. Baber, J.C. Kovacic, et al., Changes in plaque lipid content after short-term intensive versus standard statin therapy: the yellow trial (reduction in yellow plaque by aggressive lipid-lowering therapy), Journal of the American College of Cardiology 62 (2013) 21–29.
[34] J.A. Goldstein, B. Maini, S.R. Dixon, et al., Detection of lipid-core plaques by intracoronary near-infrared spectroscopy identifies high risk of periprocedural myocardial infarction, Circulation: Cardiovascular Interventions 4 (2011) 429–437.
[35] G.W. Stone, A. Maehara, J.E. Muller, et al., Plaque characterization to inform the prediction and prevention of periprocedural myocardial infarction during percutaneous coronary intervention: the canary trial (coronary assessment by near-infrared of atherosclerotic rupture-prone yellow), Journal of the American College of Cardiology: Cardiovascular Interventions 8 (2015) 927–936.
[36] J. Pu, G.S. Mintz, E.S. Brilakis, et al., In vivo characterization of coronary plaques: novel findings from comparing greyscale and virtual histology intravascular ultrasound and near-infrared spectroscopy, European Heart Journal 33 (2012) 372–383.
[37] T. Roleder, J.C. Kovacic, Z. Ali, et al., Combined NIRS and IVUS imaging detects vulnerable plaque using a single catheter system: a head-to-head comparison with OCT, EuroIntervention 10 (2014) 303–311.
[38] N. Gonzalo, J. Escaned, F. Alfonso, et al., Morphometric assessment of coronary stenosis relevance with optical coherence tomography: a comparison with fractional flow reserve and intravascular ultrasound, Journal of the American College of Cardiology 59 (2012) 1080–1089.
[39] T. Yonetsu, W. Suh, F. Abtahian, et al., Comparison of near-infrared spectroscopy and optical coherence tomography for detection of lipid, Catheter Cardiovascular Interventions 84 (2014) 710–717.
[40] S. Brugaletta, H.M. Garcia-Garcia, P.W. Serruys, et al., NIRS and IVUS for characterization of atherosclerosis in patients undergoing coronary angiography, Journal of the American College of Cardiology: Cardiovascular Imaging 4 (2011) 647–655.
[41] T. Sawada, J. Shite, H.M. Garcia-Garcia, et al., Feasibility of combined use of intravascular ultrasound radiofrequency data analysis and optical coherence tomography for detecting thin-cap fibroatheroma, European Heart Journal 29 (2008) 1136–1146.
[42] A.S. Kini, S. Motoyama, Y. Vengrenyuk, et al., Multimodality intravascular imaging to predict periprocedural myocardial infarction during percutaneous coronary intervention, Journal of the American College of Cardiology: Cardiovascular Interventions 8 (2015) 937–945.